Electronic Supplementary Material (ESI) for Physical Chemistry Chemical Physics.

Table of contents

1. Experimental Raman and SERS Spectra

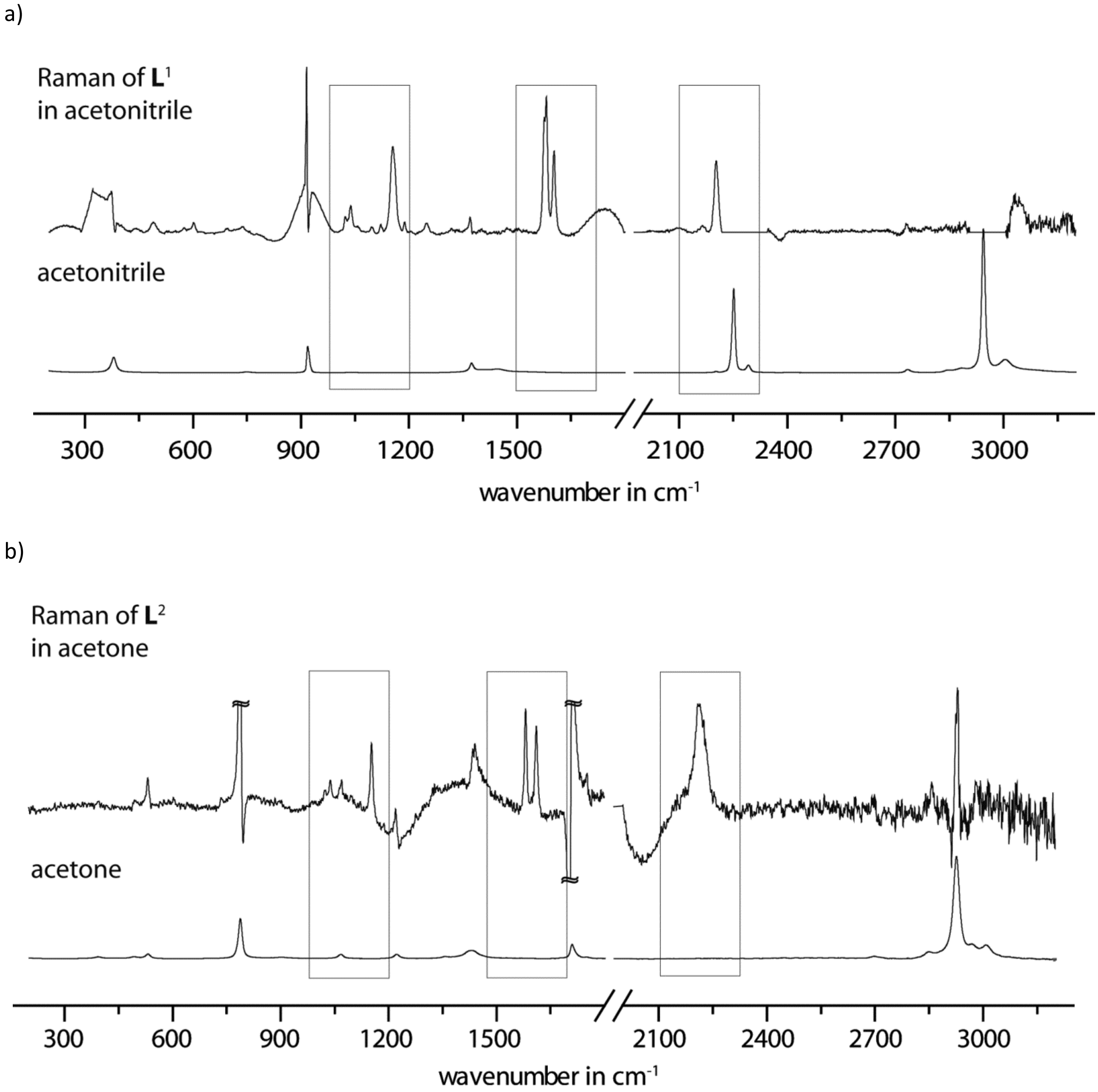

Figure-SI 1: a) Showcase overlay of a Raman spectrum for ligand a) **L**^{1} in acetonitrile and b) **L**^{2} in acetone and a spectrum of the correspondent solvent. The “derivative” like bands in the analyte spectrum have their origin in the subtraction of the solvent bands. For further investigation we have set our focus on the parts of the spectrum with a minimal superimposition (marked by grey boxes).

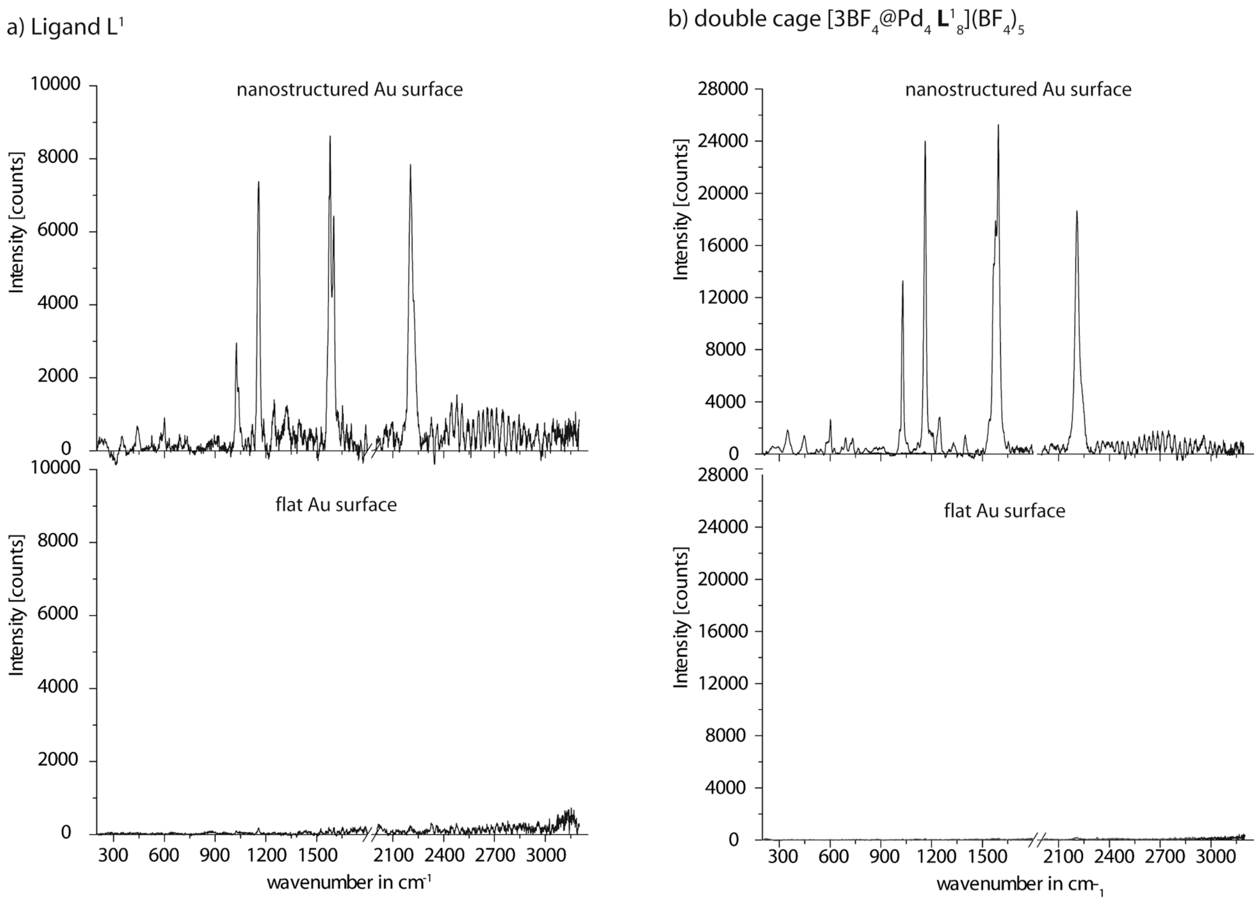

a) Ligand L^1

b) double cage $[3BF_4@Pd_4\mathbf{L}^1{}_8](BF_4)_5$

Figure-SI 2: SERS spectra of deposition of the substrate a) ligand $\mathbf{L}^1$ and b) double cage $[3BF_4@Pd_4\mathbf{L}^1{}_8](BF_4)_5$ on a nanostructured and on an flat gold surface showing an enhancement of the signals when the nanostructured Au surface is used. Recording time was 10 s.

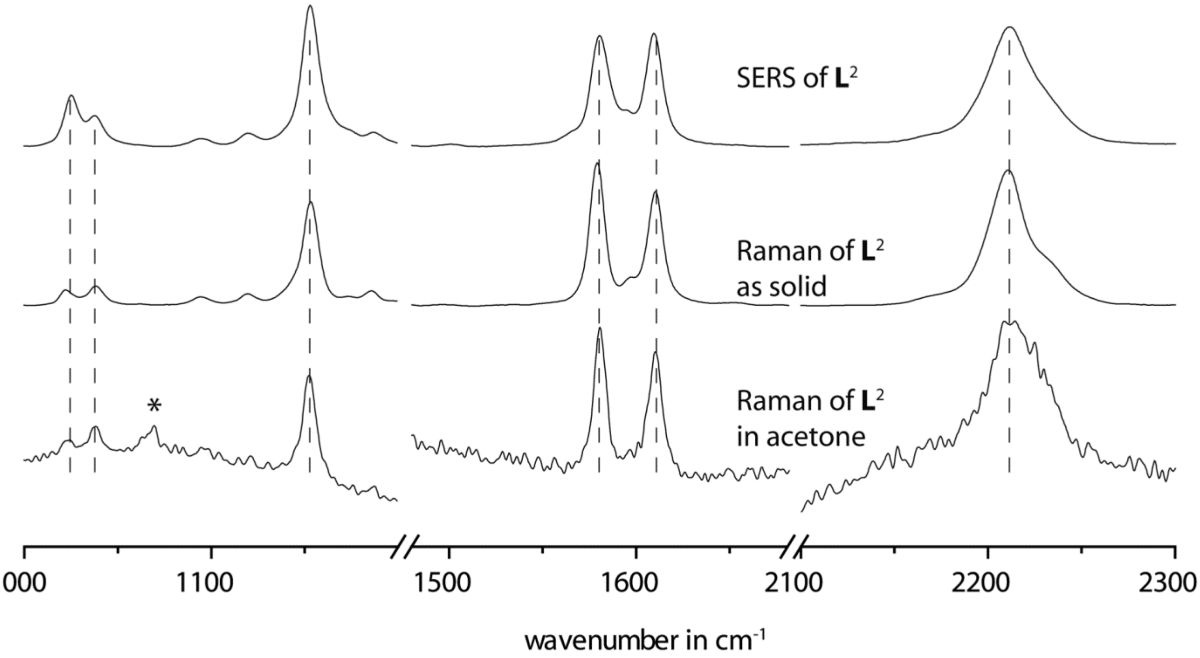

Figure-SI 3: Experimental Raman spectra in solution (acetone) and of a solid for the ligand **L**^{2}and SERS spectra on an Au coated surface in the ranges of 1000-1200 cm^{-1}, 1480-1680 cm^{-1} and 2100-2300 cm^{-1}. The auxiliary dashed lines are referenced to the middle spectrum. * denotes the residual signal arising from solvent subtraction.

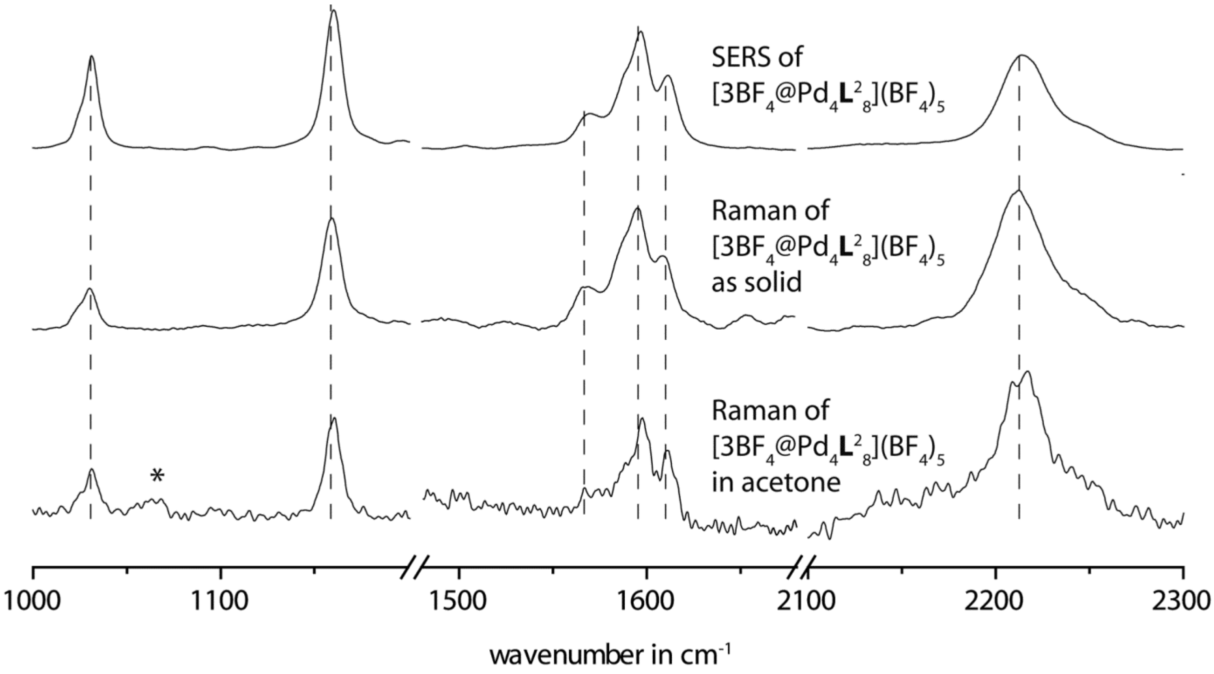

Figure-SI 4: Experimental Raman spectra in solution (acetone) and of a solid for the double cage [3BF$_4$@Pd$_4$**L**$^2{}_8$](BF$_4$)$_5$ and SERS spectra on an Au coated surface in the ranges of 1000-1200 cm^{-1}, 1480-1680 cm^{-1} and 2100-2300 cm^{-1}. The auxiliary dashed lines are referenced to the middle spectrum. * denotes the residual signal arising from solvent subtraction.

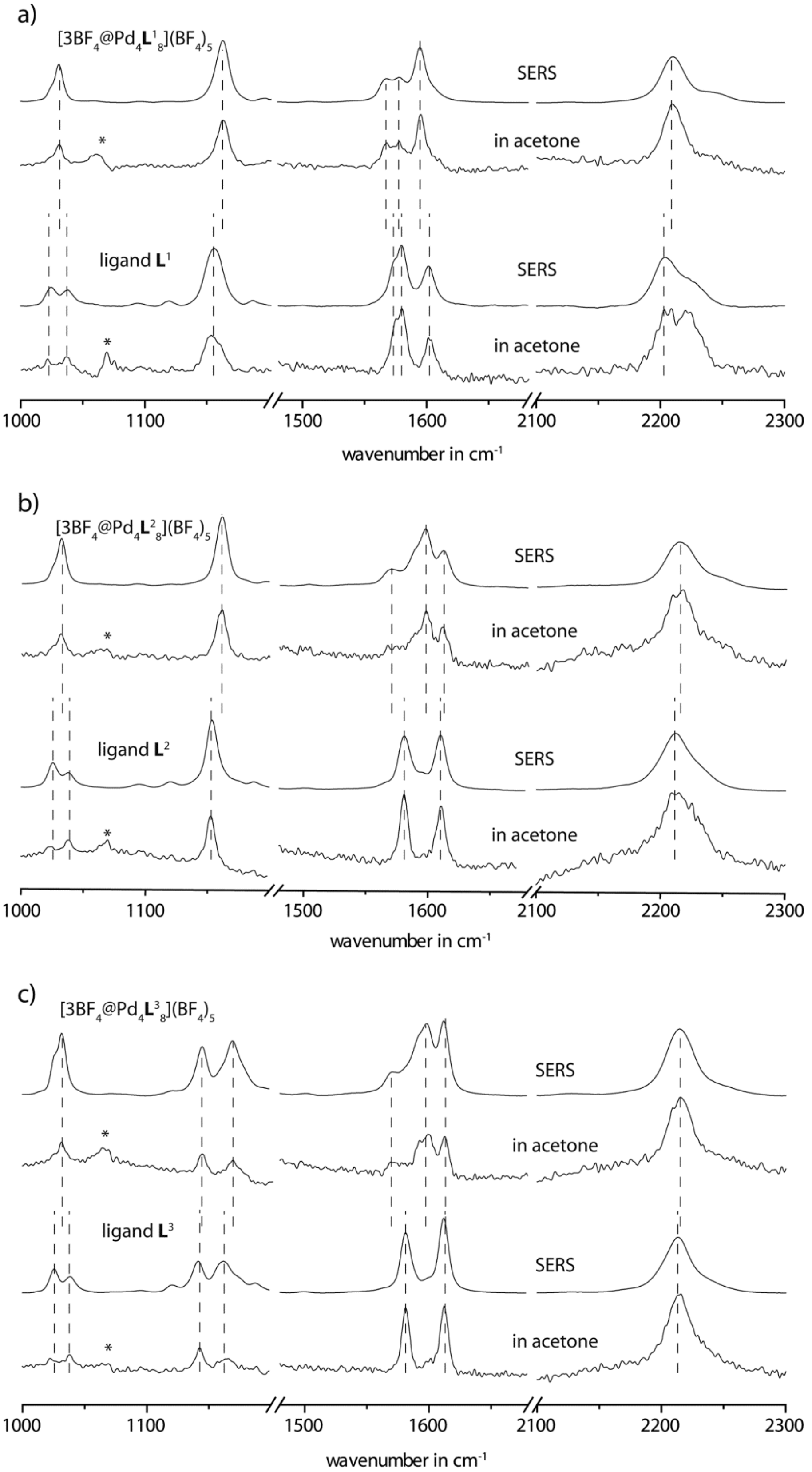

Figure-SI 5: Comparison between the experimental Raman spectra in solution (acetone) of the ligands **L**^{n} and their corresponding double cages [3BF$_4$@Pd$_4$**L**$^n{}_8$](BF$_4$)$_5$ with a) n = 1, b) n= 2 and c) n=3 and SERS spectra on an Au coated surface in the ranges of 1000-1200 cm^{-1}, 1480-1680 cm^{-1} and 2100-2300 cm^{-1}. * denotes the residual signal arising from solvent subtraction.

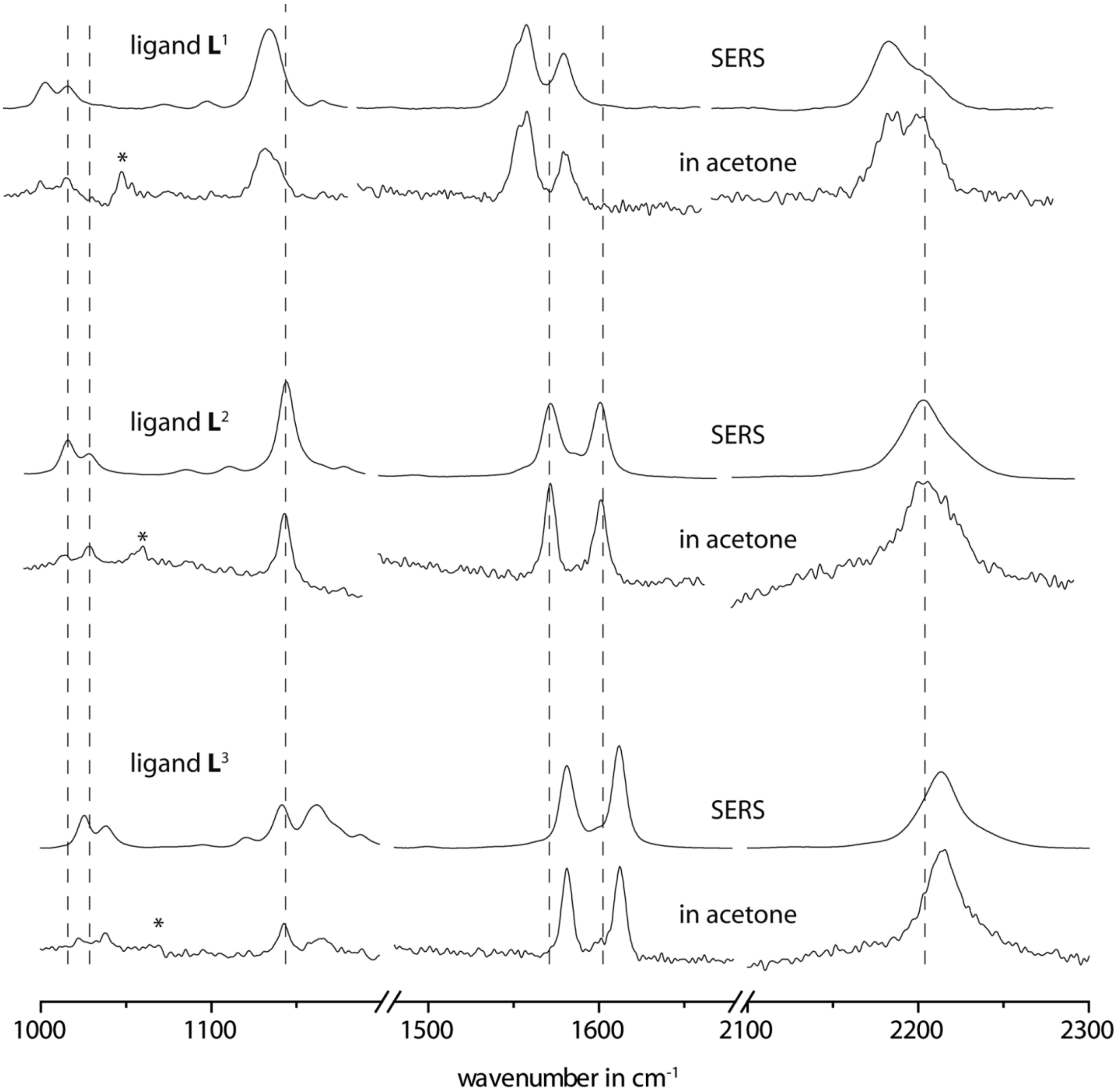

Figure-SI 6: Experimental Raman spectra in solution (acetone) of the ligands $\mathbf{L}^{1\text{-}3}$ and SERS spectra on an Au coated surface in the ranges of 1000-1200 cm^{-1}, 1480-1680 cm^{-1} and 2100-2300 cm^{-1}. The auxiliary dashed lines are referenced to the spectrum of ligand $\mathbf{L}^2$. * denotes the residual signal arising from solvent subtraction.

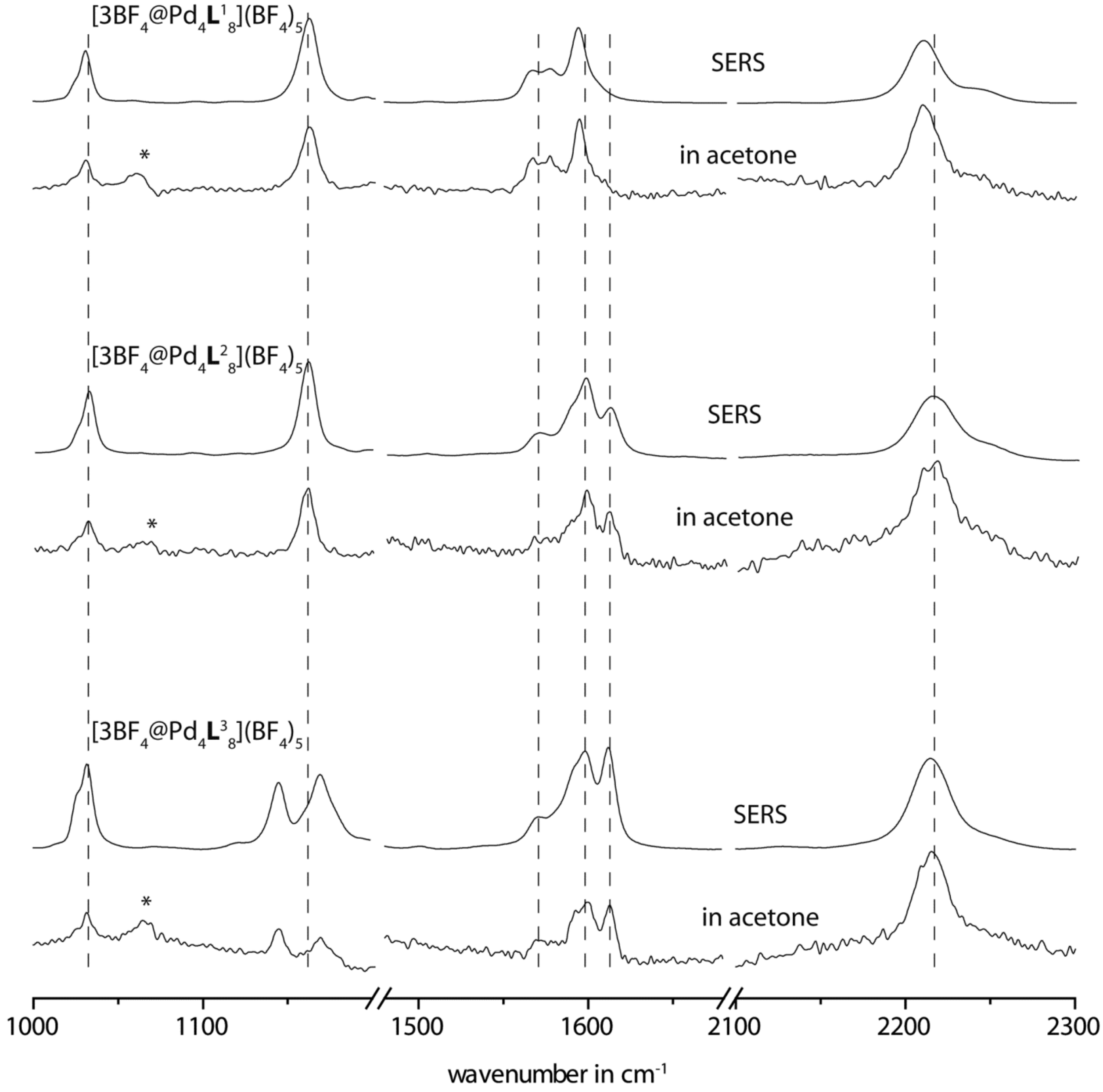

Figure-SI 7: Experimental Raman spectra in solution (acetone) of the self-assembled cages $[3BF_4@Pd_4\mathbf{L}^n{}_8](BF_4)_5$ with n = 1-3 and SERS spectra on an Au coated surface in the ranges of 1000-1200 cm^{-1}, 1480-1680 cm^{-1} and 2100-2300 cm^{-1}. The auxiliary dashed lines are referenced to the spectrum of ligand $[3BF_4@Pd_4\mathbf{L}^2{}_8](BF_4)_5$. * denotes the residual signal arising from solvent subtraction.

Table 1 Vibrational experimental wavenumbers and intensities for the ligands **L**^{n} and the cages [$3BF_4@Pd_4$**L**$^n{}_8$]$(BF_4)_5$ with n = 1-3.

Experimental frequencies[a] for the ligand **L**^{1}in cm^{-1}		Experimental frequencies[a] for the cage [$3BF_4@Pd_4$**L**$^1{}_8$]$(BF_4)_5$ in cm^{-1}		Experimental frequencies[a] for the ligand **L**^{2} in cm^{-1}		Experimental frequencies[a] for the cage [$3BF_4@Pd_4$**L**$^1{}_8$]$(BF_4)_5$ in cm^{-1}		Experimental frequencies[a] for the ligand **L**^{3} in cm^{-1}		Experimental frequencies[a] for the cage [$3BF_4@Pd_4$**L**$^3{}_8$]$(BF_4)_5$ in cm^{-1}	
Raman	SERS	Raman	SERS	Raman	SERS	Raman	SERS	Raman	SERS	Raman	SERS
	347 w		348 w		445 w				609 w		610 m
	449 w		441 w		527 vw						668 vw
	602 w		600 w		600 w		599 w		692 vw		691 vw
1022 m	1025 m	1031 m	1031 s				668 w		732 w		733 w
1037 m	1038 m				690 vw		689 w	1022 w	1025 m		
1154 s	1156 vs	1163 s	1163 vs		733 w		733 w	1038 w	1038 m	1031 m	1031 vs
	1187 vw		1197 vw	1024 w	1025 m				1121 sh		1122 sh
	1248 w		1248 w	1038 m	1037 m	1031 m	1031 s	1142 m	1142 m	1145 m	1145 s
1576 sh	1575 vs	1568 m	1568 m		1094 vw			1166 w	1162 m	1169 m	1169 s
1580 vs	1580 vs	1578 m	1578 m		1120 w				1187 sh		1194 sh
1601 s	1602 s	1595 s	1595 vs	1152 s	1153 vs	1161 s	1160 vs		1276 vw		
2203 vs	2204 vs	2210 vs	2210 vs		1172 w				1298 w		1300 w
					1187 w		1197 vw		1330 w		1330 w
					1276 w		1276 vw			1593 sh	1571 sh
					1302 vw		1305 w	1581 vs	1581 vs	1599 s	1598 vs
					1326 vw		1332 w	1612 vs	1612 vs	1613 s	1612 vs
				1581 vs	1580 vs		1570 m	2216 vs	2213 vs	2215 vs	2215 vs
					1595 w	1598 s	1597 vs				
				1610 vs	1610 vs	1611 m	1611 s				
				2209 vs	2212 vs	2214 vs	2214 vs				

Experimental intensity description: vs = very strong; s = strong; m = medium; w = weak; vw = very weak; sh = shoulder.

[a] This work.

2. Calculated vibrational spectra for the ligands L^n with n =1-3

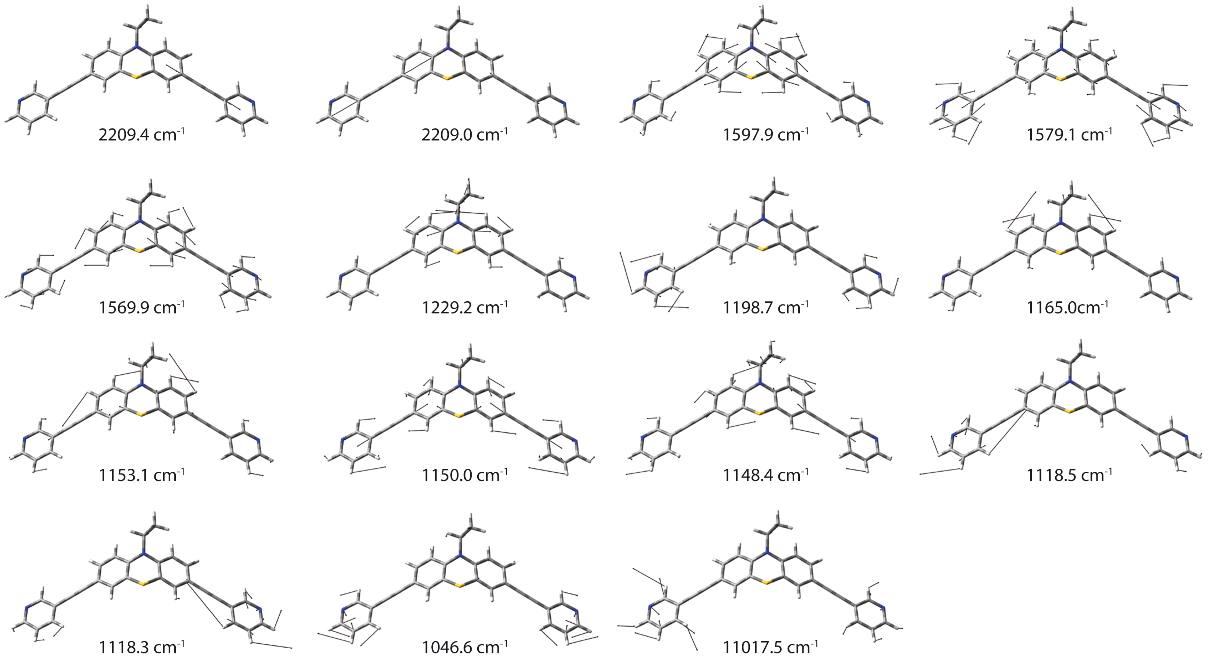

Figure-SI 8: Calculated vibrational modes with the highest intensity for the ligand $\mathbf{L}^1$.

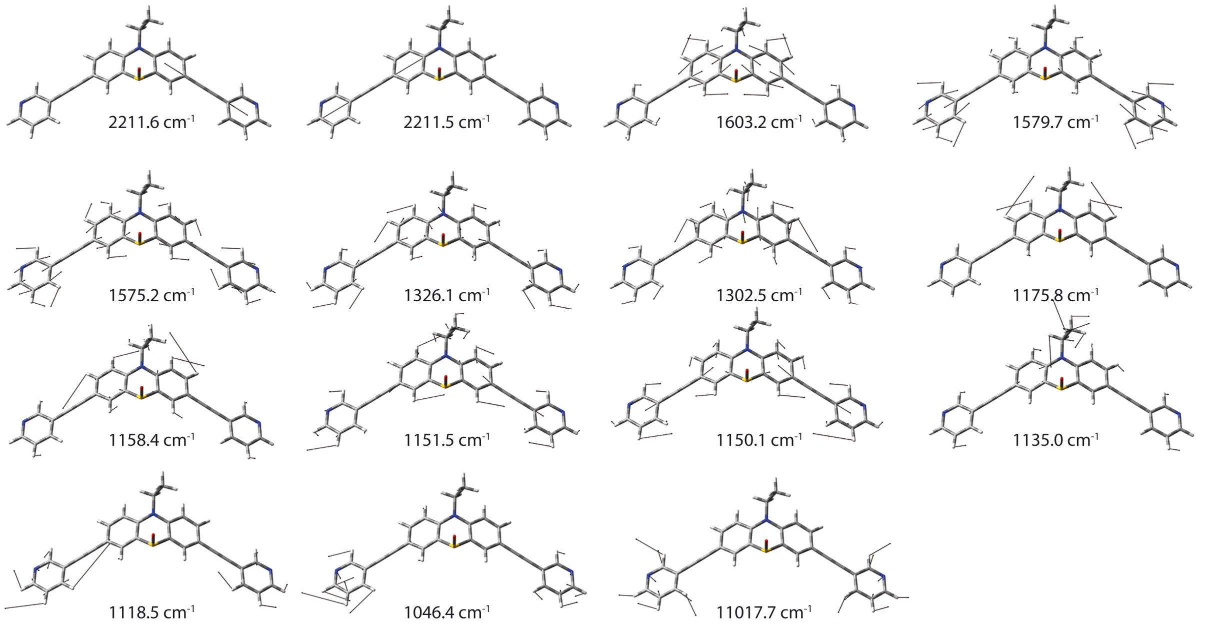

Figure-SI 9: Calculated vibrational modes with the highest intensity for the ligand $\mathbf{L}^2$ with the oxygen in axial position.

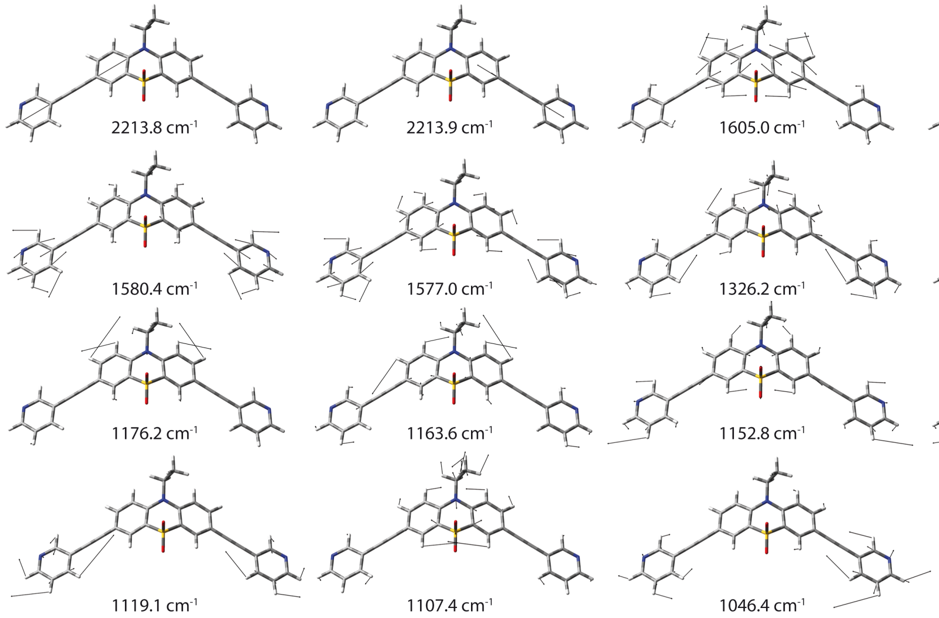

Figure-SI 10: Calculated vibrational modes with the highest intensity for the ligand **L**^{3}.

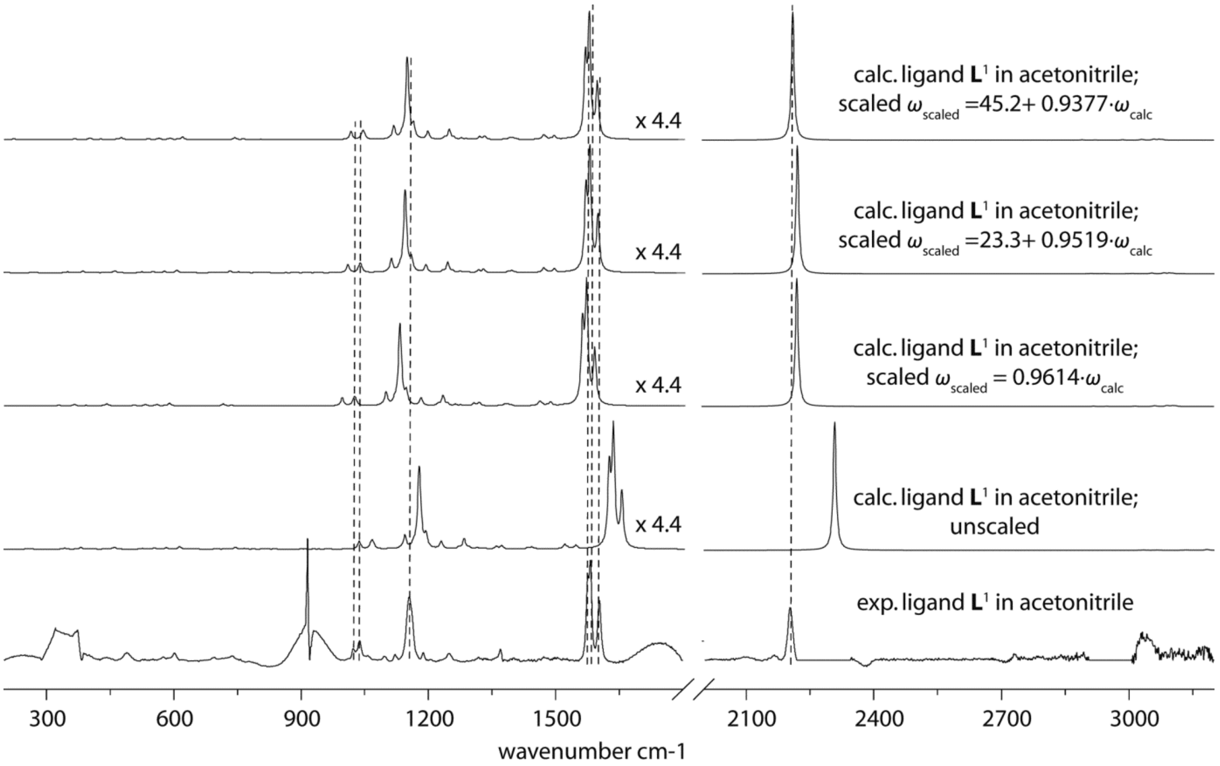

Figure-SI 11: Scaling methods for the calculated spectrum of the ligand **L^1.**

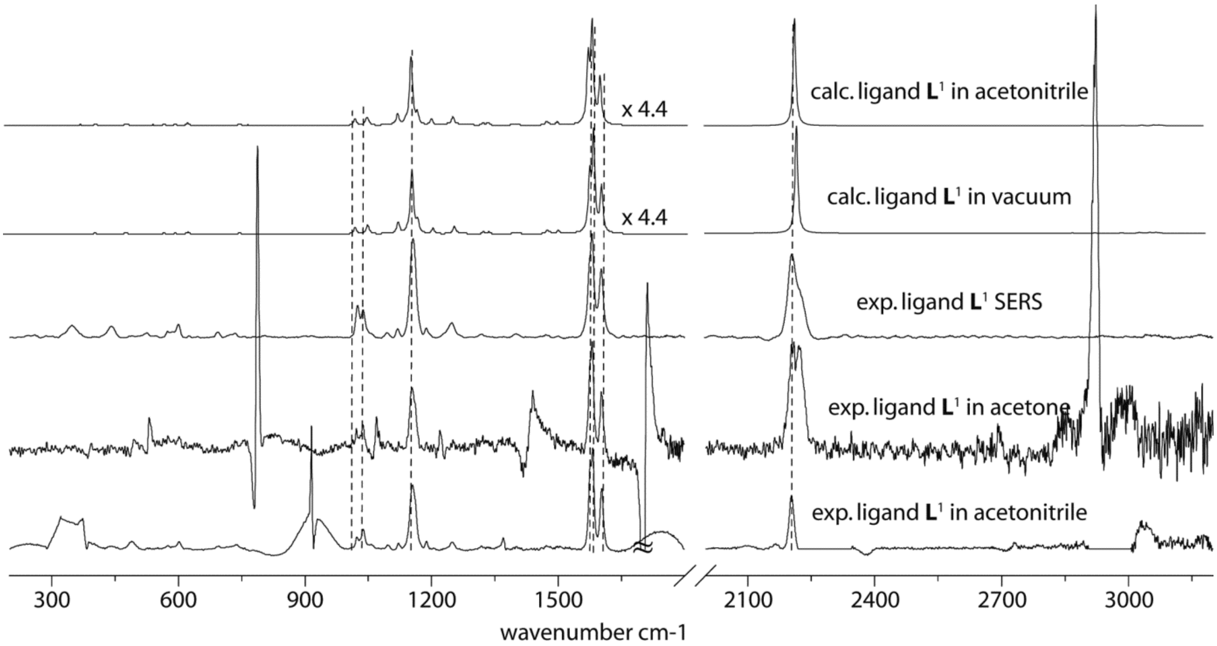

Figure-SI 12: Calculated vibrational spectra using a solvent (acetonitrile) and in vacuum for the ligand **L**^{1} vs. experimental spectra in solution (acetonitrile and acetone) and on Au surface (SERS). The range 200-1800 cm^{-1} of the calculated spectra was enlarged by a factor of 4.4.

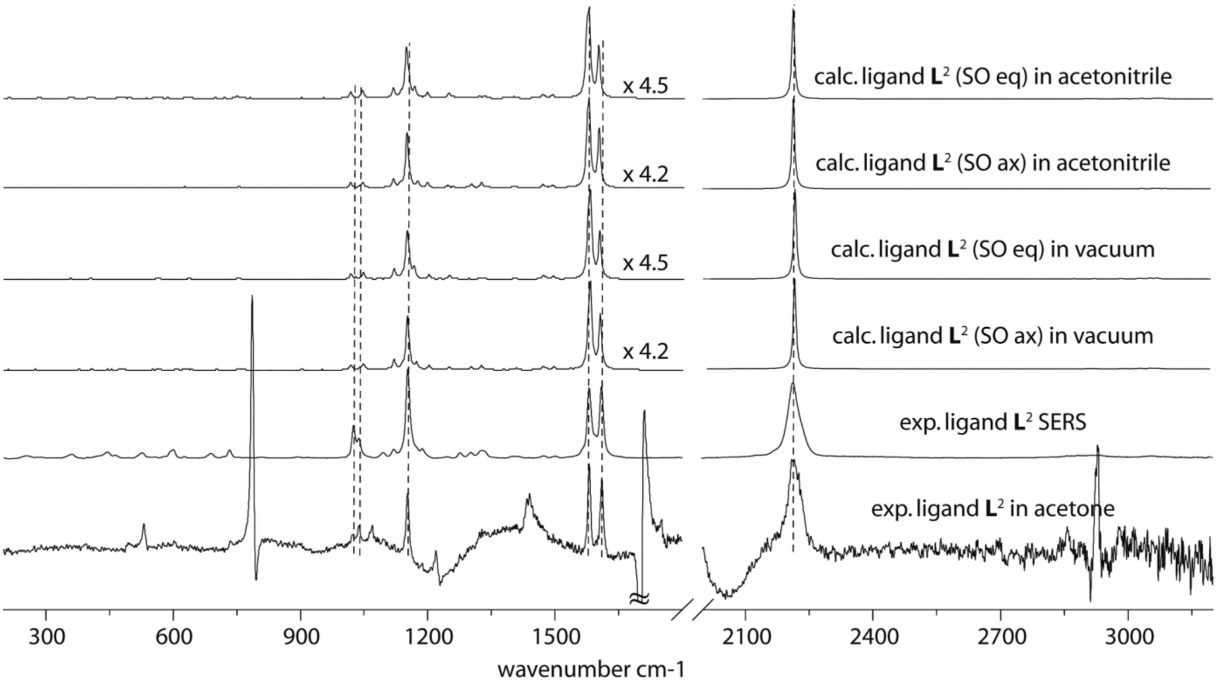

Figure-SI 13: Calculated vibrational spectra using a solvent (acetonitrile) and in vacuum for the ligand **L**^{2} with variation of the oxygen position vs. experimental spectra in solution (acetone) and on Au surface (SERS). The range 200-1800 cm^{-1} of the calculated spectra was enlarged by a factor of 4.2 for the oxygen in axial position and 4.5 for equatorial position.

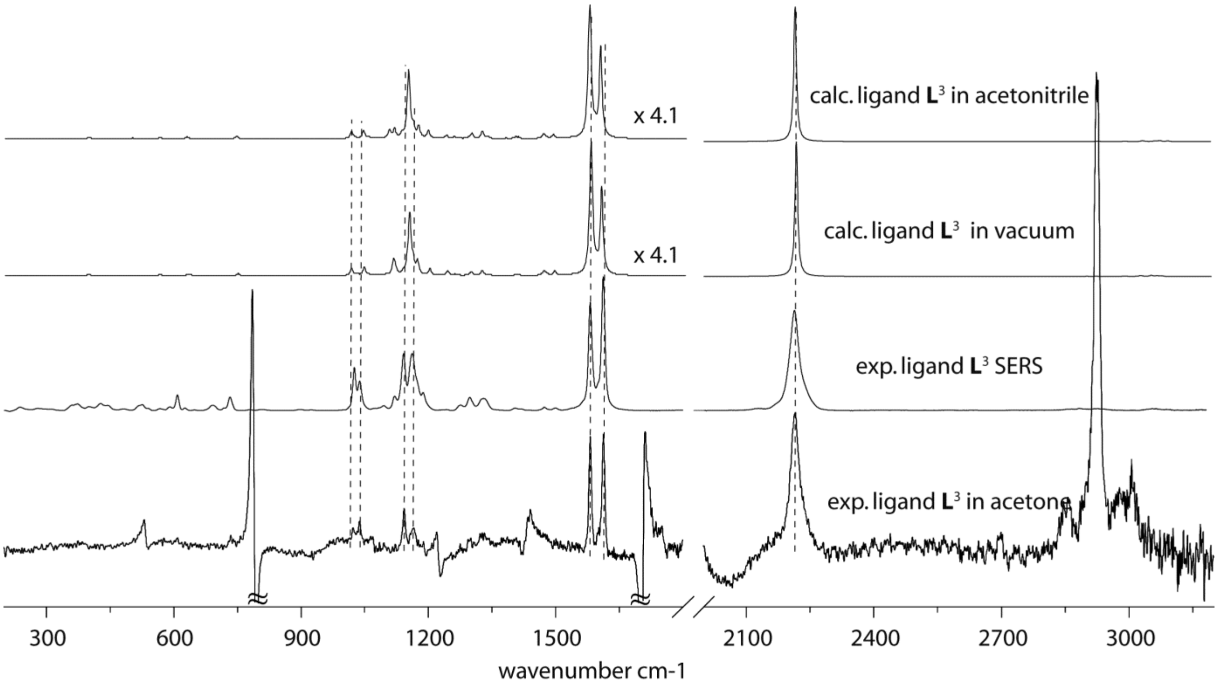

Figure-SI 14: Calculated vibrational spectra using a solvent (acetonitrile) and in vacuum for the ligand $\mathbf{L}^3$ vs. experimental spectra in solution (acetone) and on Au surface (SERS). The range 200-1800 cm^{-1} of the calculated spectra was enlarged by a factor of 4.1.

3. Calculated vibrational spectra for the cages $[3BF_4@Pd_4L^n_8](BF_4)_5$ with n =1-3

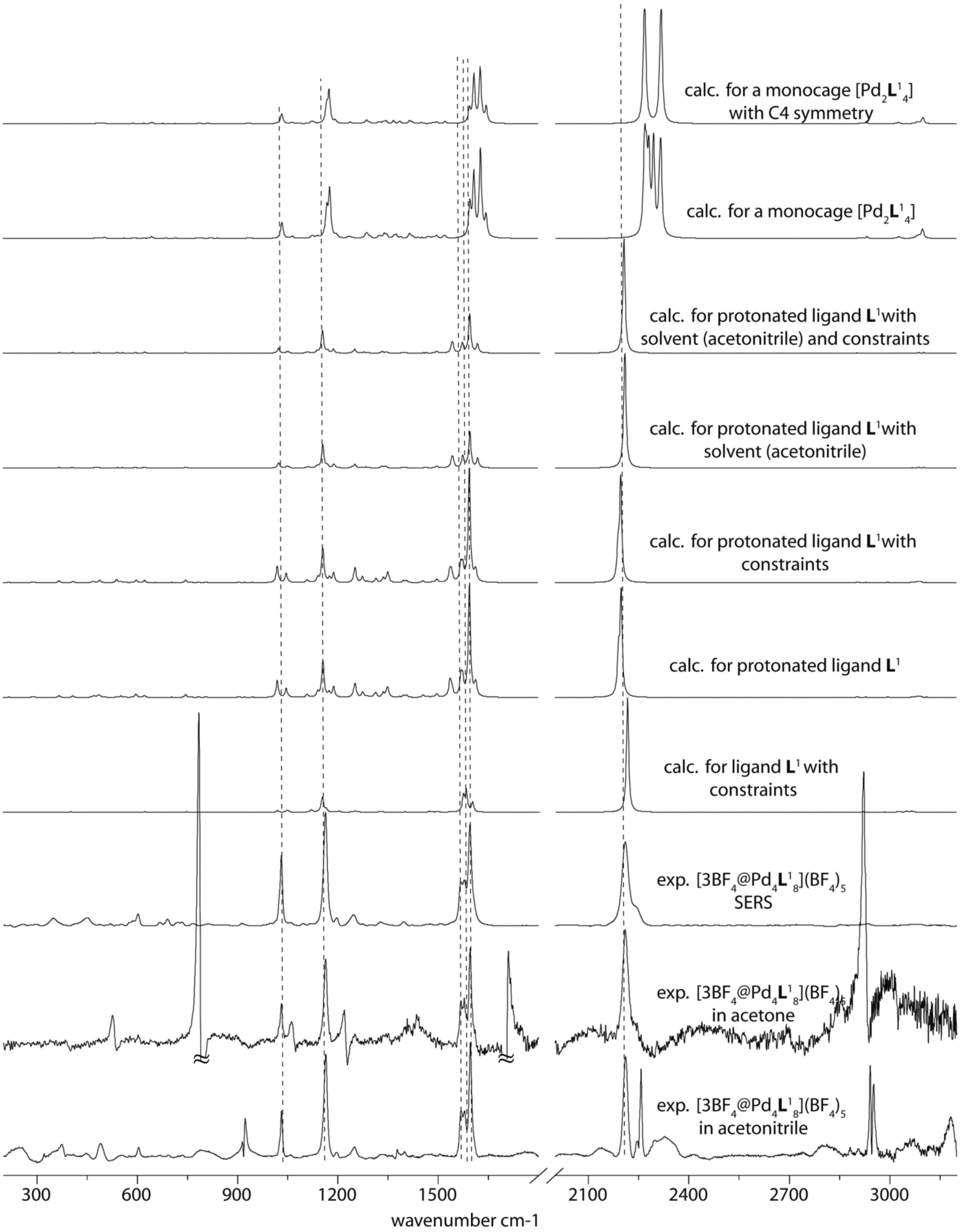

Figure-SI 15: Calculated vibrational spectra using different approaches such as i) defined distance between the pyridine atoms (abbr. constraints), ii) protonation of the ligand at the pyridine arms, iii) combination of defined distance and protonation, iv) protonation and solvation (acetonitrile), v) combination of defined distance, protonation and solvation, vi) a model of a monomeric cage $[Pd_2\mathbf{L}^1_4]$ and vii) a model of a monomeric cage $[Pd_2\mathbf{L}^1_4]$ with a C4 symmetry as a simplified model for the double cage $[3BF_4@Pd_4\mathbf{L}^1_8](BF_4)_5$ vs. experimental spectra in solution (acetonitrile and acetone) and in solid state (SERS).

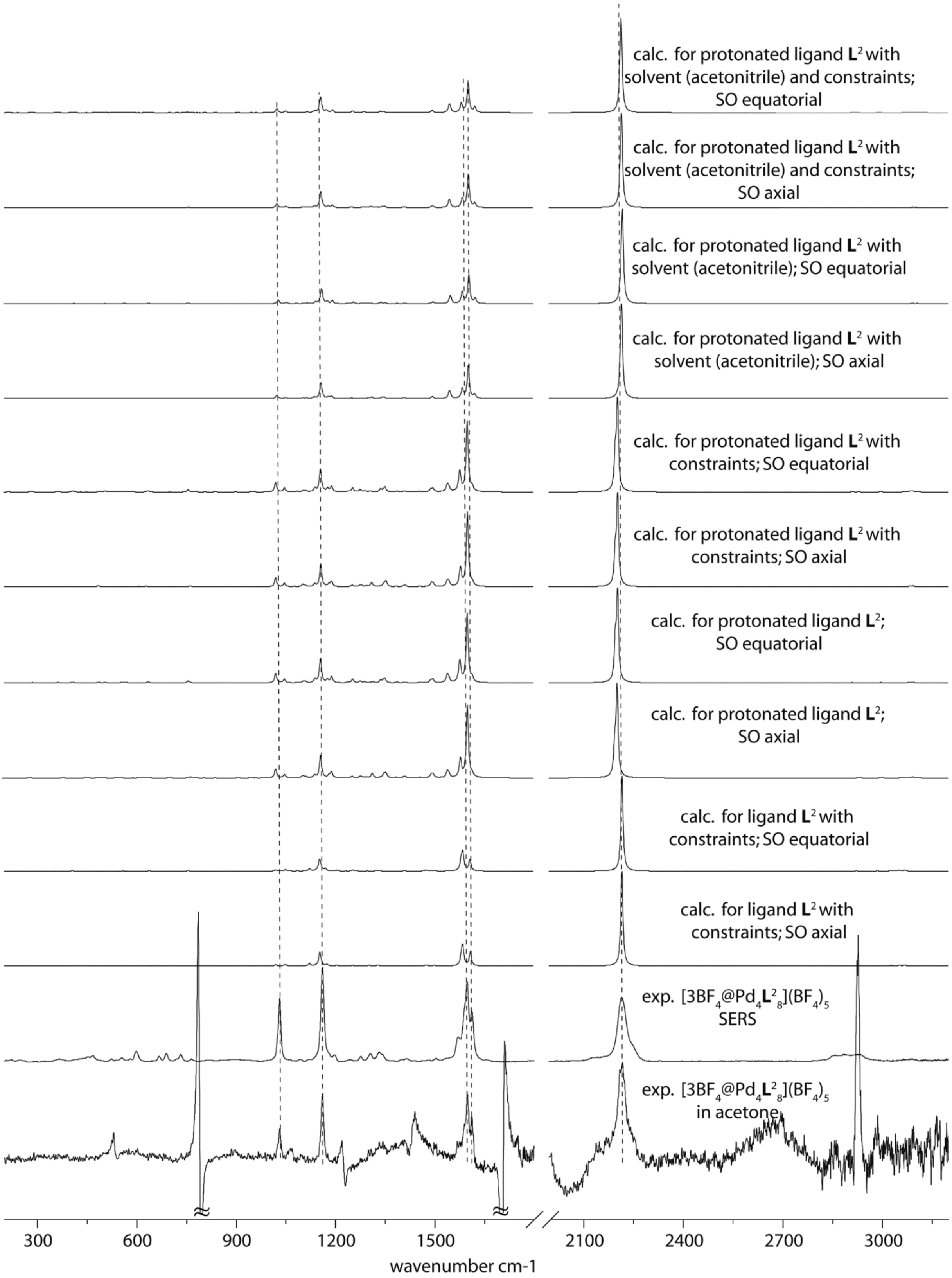

Figure-SI 16: Calculated vibrational spectra using different approaches such as i) defined distance between the pyridine atoms (abbr. constraints), ii) protonation of the ligand at the pyridine arms, iii) combination of defined distance and protonation, iv) protonation and solvation (acetonitrile), v) combination of defined distance, protonation and solvation as a simplified model for the double cage $[3BF_4@Pd_4\mathbf{L}^2_8](BF_4)_5$ vs. experimental spectra in solution (acetone) and in solid state (SERS). The calculations were done for two possible positions of the oxygen atom (equatorial and axial orientation).

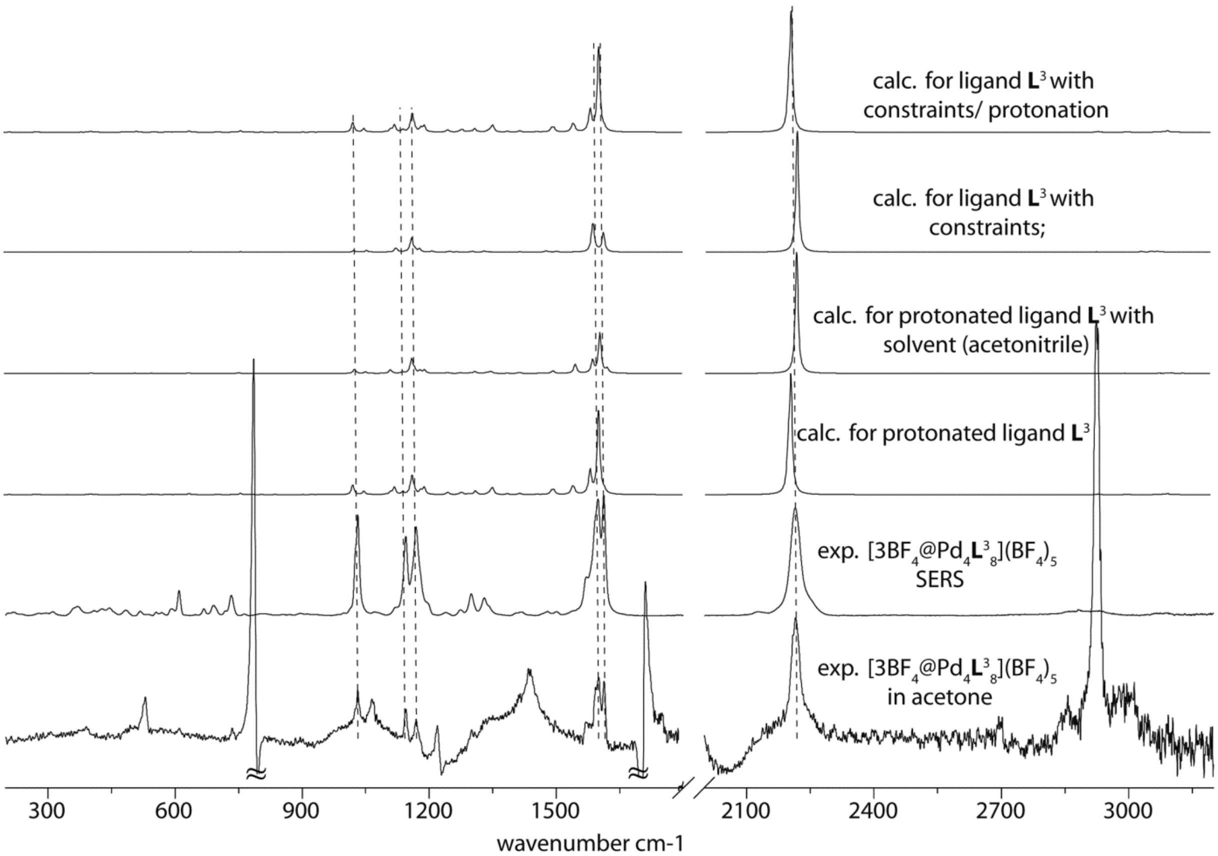

Figure-SI 17: Calculated vibrational spectra using different approaches such as i) protonation of the ligand at the pyridine arm, ii) combination of protonation and solvation (acetonitrile), iii) defined distance between the pyridine atoms (abbr. constraints) and iv) combination of defined distance and protonation as a simplified model for the double cage $[3BF_4@Pd_4\mathbf{L}^3_8](BF_4)_5$ vs. experimental spectra in solution (acetone) and in solid state (SERS).

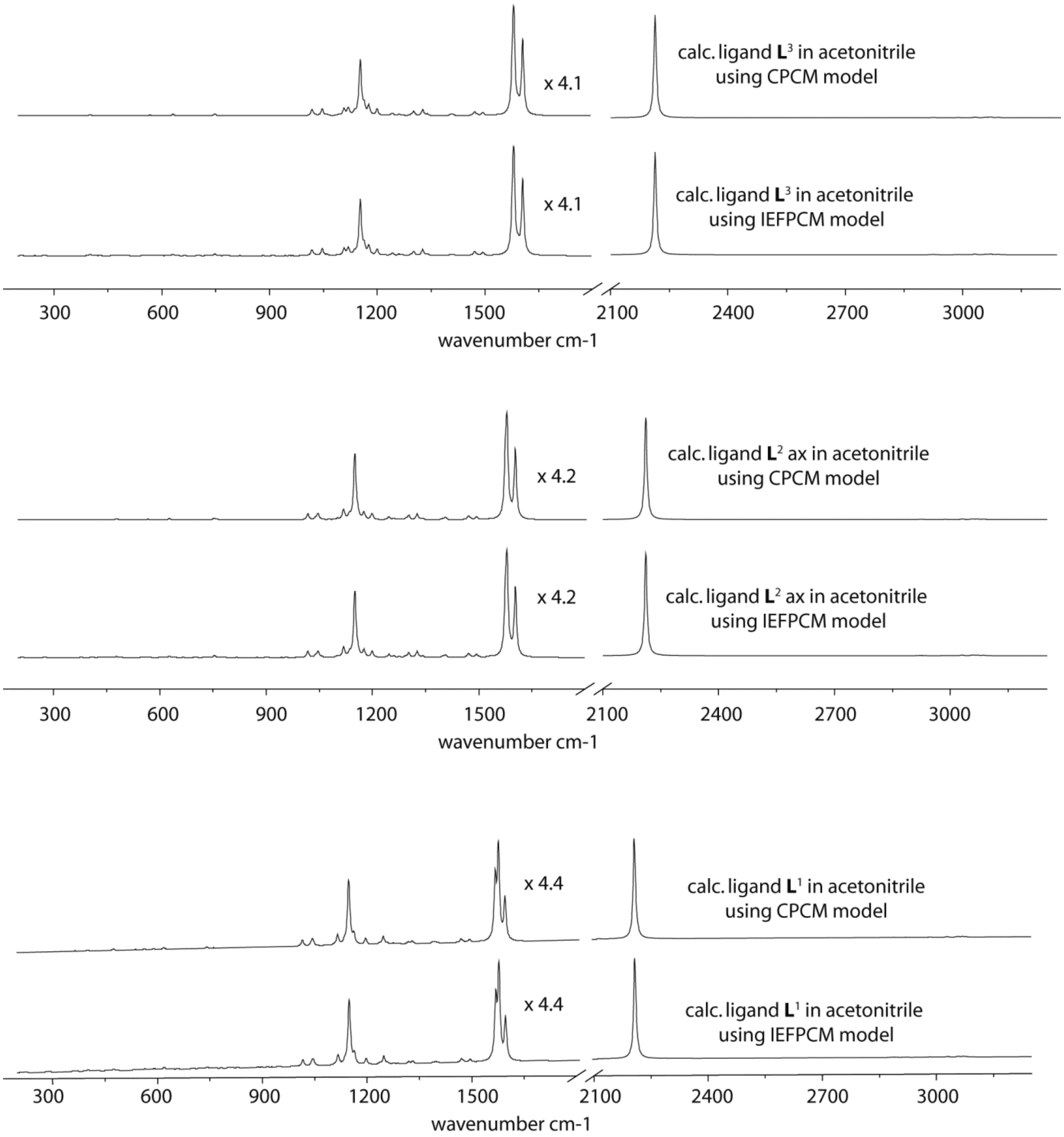

Figure-SI 18: Calculated vibrational spectra using different solvation models[1] for the ligands $\mathbf{L}^n$ with n = 1, 2 (O = axial) and 3. CPCM (conductor polarizable continuum model)[2] and the IEFPCM (integral equation formalism polarizable continuum model)[3].

---

[1] J. Tomasi, B. Mennucci, R. Cammi, *Chem. Rev.,* 2005, **105**, 2999.

[2] V. Barone and M. Cossi, "Quantum calculation of molecular energies and energy gradients in solution by a conductor solvent model," *J. Phys. Chem. A*, 1998, **102**, 1995; M. Cossi, N. Rega, G. Scalmani, and V. Barone, "Energies, structures, and electronic properties of molecules in solution with the C-PCM solvation model," *J. Comp. Chem.*, 2003, **24**, 669.

[3] G. Scalmani and M. J. Frisch, "Continuous surface charge polarizable continuum models of solvation. I. General formalism," *J. Chem. Phys.*, 2010, **132**, 114110.